ISSN 1070-3284, Russian Journal of Coordination Chemistry, 2017, Vol. 43, No. 12, pp. 816–827. © Pleiades Publishing, Ltd., 2017.
Original Russian Text © A.V. Piskunov, I.N. Meshcheryakova, G.K. Fukin, I.V. Smolyaninov, N.T. Berberova, 2017, published in Koordinatsionnaya Khimiya, 2017, Vol. 43, No. 12, pp. 718–729.

Syntheses, Structures, and Electrochemical Properties of the Tin(IV) Complexes Based on the 2-Hydroxy-4-*N*-(Phenyl)-3,6-Di-*tert*-Butyl-*p*-Iminobenzoquinone Ligand

A. V. Piskunov[a], *, I. N. Meshcheryakova[a], G. K. Fukin[a], I. V. Smolyaninov[b, c], **, and N. T. Berberova[b]

[a] *Razuvaev Institute of Organometallic Chemistry, Russian Academy of Sciences, ul. Tropinina 49, Nizhni Novgorod, 603600 Russia*

[b] *Astrakhan State Technical University, Astrakhan, Russia*

[c] *Southern Scientific Center, Russian Academy of Sciences, Rostov-on-Don, Russia*

**e-mail: pial@iomc.ras.ru*

***e-mail: ivsmolyaninov@gmail.com*

Received June 30, 2017

Abstract—A series of the new tin(IV) complexes based on the 2-hydroxy-4-*N*-(phenyl)-3,6-di-*tert*-butyl-*p*-iminobenzoquinone ligand (LH) containing various hydrocarbon substituents R at the metal atom (R = Me, Et, ^{n}Bu, ^{t}Bu, and Ph) is synthesized. The structures of the synthesized compounds were determined by elemental analysis, IR spectroscopy, and ^{1}H and ^{119}Sn NMR spectroscopy. The X-ray diffraction analyses are carried out for the $LSnPh_3$ (**I**) and L_2SnEt_2 (**IV**) complexes (CIF files CCDC no. 1557840 (**I**) and 1557839 (**IV**)). The main electrochemical characteristics in a solution are obtained for the whole series by cyclic voltammetry.

Keywords: oxy-*p*-iminobenzoquinone, tin, X-ray diffraction analysis, cyclic voltammetry, non-transition metal complexes, redox-active ligands

DOI: 10.1134/S1070328417120077

INTRODUCTION

Specific features of the behavior of organometallic and coordination compounds in chemical processes are governed by the nature of both the metal center and organic ligands. The latter play an important role. In particular, this is urgent for the compounds based on redox-active ligands directly involved in the chemical reaction undergoing oxidation or reduction by various agents and remained bound to the metal. These compounds are very interesting from the viewpoint of studying the redox processes involving them, since they allow the fine variation of their oxidative or reductive abilities to be performed due to the introduction of diverse groups into the ligand. In turn, the oxidative or reductive abilities make it possible to conduct the redox reaction in the rigidly necessary direction under specified conditions [1–5]. The most part of studies performed to the present time concerns the quinone and iminoquinone metal complexes containing the redox-active ligand in the reduced form [1–5]. Correspondingly, the ligands are oxidized during the reaction, and this process is often irreversible. There are considerably less examples for the reactions involving the compounds containing the neutral form of the quinone (iminoquinone) ligand [6, 7]. We have recently synthesized the series of the tin(IV) complexes based on 2-hydroxy-3,6-di-*tert*-butyl-*p*-benzoquinone (L'H) and studied their electrochemical behavior in a solution [8, 9]. These compounds act in redox processes as oxidants, which makes it possible to extend the range of reactants and reactions involving metal complexes with redox-active ligands. This work is devoted to the study of the tin(IV) compounds containing the 2-oxy-3,6-di-*tert*-butyl-*p*-iminobenzoquinone ligand (L). Unlike its analog, 2-oxy-*p*-iminobenzoquinone contains the substituted nitrogen atom, which allows one to control the steric properties and redox potential of the ligand depending on the used substituent at the nitrogen atom.

EXPERIMENTAL

The reagents used in the work were synthesized according to known procedures: LH [10] and $ClSnMe_3$, $ClSnPh_3$, Cl_2SnMe_2, Cl_2SnEt_2, $Cl_2Sn(^{n}Bu)_2$, $Cl_2Sn(^{t}Bu)_2$, and Cl_2SnPh_2 [11].

NMR spectra were detected in a $CDCl_3$ solution at 20°C on a Bruker Avance III instrument (400 MHz) using tetramethylsilane as an internal standard. IR spectra were recorded on an FSM-1201 FT-IR spectrometer in Nujol in KBr cells.

The electrochemical potentials of the studied compounds were measured by cyclic voltammetry (CV) in a three-electrode cell with an IPC-pro potentiostat in CH_2Cl_2 and MeCN under an argon atmosphere. The working electrode was a stationary glassy carbon (GC) electrode with a diameter of 2 mm, and a platinum

plate (S = 18 mm^2) served as the auxiliary electrode. The reference electrode (Ag/AgCl/KCl) with a water-impervious membrane was used. The concentration of the studied compounds was 0.002–0.003 mol/L. The number of electrons transferred in the course of the electrode process was estimated relative to ferrocene used as the standard. The potential sweep was 0.2 V/s. The supporting electrolyte was 0.1 M Bu_4NClO_4 (99%, Acros) doubly recrystallized from aqueous EtOH and dried in vacuo (48 h) at 50°C.

All experiments involving the synthesized complexes were carried out in the presence of air moisture and oxygen.

Synthesis of the complexes. Potassium hydroxide (0.056 g, 1 mmol) was added to a solution of 2-hydroxy-4-*N*-(phenyl)-3,6-di-*tert*-butyl-*p*-iminobenzoquinone (0.311 g, 1 mmol) in methanol (20 mL). The reaction mixture was magnetically stirred for 20 min. The color of the solution changed from red to saturated violet, indicating the formation of potassium salt LK [8]. The corresponding tin(IV) organochloride (1 mmol in the case of $ClSnPh_3$ and $ClSnMe_3$ or 0.5 mmol for Cl_2SnMe_2, Cl_2SnEt_2, $Cl_2Sn(^nBu)_2$, $Cl_2Sn(^tBu)_2$, and Cl_2SnPh_2) was added to the obtained salt with stirring. The formation of the complexes was accompanied by a change in the color of the solution from saturated violet to vinous. The reaction mixture was kept at –18°C for 24 h. The complexes were isolated as finely crystalline vinous-colored powders. All obtained compounds were resistant to air moisture and oxygen both in the solid state and in the solution.

Complex $LSnPh_3$ (**I**): the yield was 0.467 g (71%).

For $C_{38}H_{39}NO_2Sn$

anal. calcd., %	C, 69.11	H, 5.95	N, 2.12	Sn, 17.97
Found, %	C, 69.18	H, 5.99	N, 2.09	Sn, 17.90

^{1}H NMR (400 MHz), δ, ppm: 1.10 (s, 9H, $CH_3(^tBu)$), 1.59 (s, 9H, $CH_3(^tBu)$), 6.69–6.73 (s, 1H, $CH_{quinone}$ + m, 2H, CH(Ph)), 7.37–7.43 (m, 12H, CH(Ph)), 7.77–7.82 (m, 6H, CH(Ph)).

IR (ν, cm^{-1}): 1583 s, 1549 m, 1516 m, 1477 m, 1430 m, 1358 s, 1338 s, 1293 s, 1265 m, 1219 m, 1171 s, 1073 s, 1024 w, 1010 w, 998 w, 962 w, 931 w, 912 m, 904 m, 853 w, 834 w, 817 w, 795 w, 765 w, 734 s, 723 s, 695 s, 656 w, 628 m, 600 w, 575 w, 548 w.

Complex $LSnMe_3$ (**II**): analytically pure complex **II** was obtained in a yield of 0.27 g (57%).

For $C_{23}H_{33}NO_2Sn$

anal. calcd., %	C, 58.25	H, 7.01	N, 2.95	Sn, 25.03
Found, %	C, 58.30	H, 7.05	N, 2.91	Sn, 24.99

^{1}H NMR (400 MHz), δ, ppm: 0.42 (s, 9H, Me), 1.12 (s, 9H, $CH_3(^tBu)$), 1.53 (s, 9H, $CH_3(^tBu)$), 6.68 (s, 1H, $CH_{quinone}$), 6.73 (m, 2H, CH(Ph)), 7.30–7.36 (m, 3H, CH(Ph)).

IR (ν, cm^{-1}): 1589 s, 1557 m, 1528 s, 1480 s, 1392 m, 1361 s, 1336 s, 1301 s, 1270 s, 1224 s, 1198 w, 1177 m, 1071 w, 1009 w, 956 w, 919 m, 908 w, 898 w, 836 w, 819 w, 795 w, 763 m, 737 w, 697 m, 654 w, 617 w, 579 w, 540 w, 529 w, 513 w.

Complex L_2SnMe_2 (**III**): analytically pure complex **III** was obtained in a yield of 0.335 g (87%).

For $C_{42}H_{54}N_2O_4Sn$

anal. calcd., %	C, 65.55	H, 7.07	N, 3.64	Sn, 15.42
Found, %	C, 65.59	H, 7.10	N, 3.61	Sn, 15.38

^{1}H NMR (400 MHz), δ, ppm: 0.65 (s, 6H, Me), 1.14 (s, 18H, $CH_3(^tBu)$), 1.61 (s, 18H, $CH_3(^tBu)$, 6.72 (s, 2H, $CH_{quinone}$), 6.73 (m, 4H, CH(Ph)), 7.10 (m, 2H, CH(Ph)), 7.33 (m, 4H, CH(Ph)). ^{119}Sn NMR (149 MHz), δ, ppm: –165.44.

IR (ν, cm^{-1}): 1597 s, 1590 s, 1548 m, 1515 m, 1479 m, 1397 w, 1362 s, 1335 s, 1289 s, 1269 s, 1222 s, 1202 w, 1173 s, 1071 m, 1007 w, 953 w, 931 w, 919 m, 907 w, 900 w, 838 w, 820 w, 795 m, 786 m, 765 w, 739 m, 699 m, 652 w, 614 m, 606 w, 576 w, 547 w, 524 w.

Complex L_2SnEt_2 (**IV**): analytically pure complex **IV** was obtained in a yield of 0.323 g (81%).

For $C_{44}H_{58}N_2O_4Sn$

anal. calcd., %	C, 66.25	H, 7.33	N, 3.51	Sn, 14.88
Found, %	C, 66.20	H, 7.29	N, 3.50	Sn, 14.91

^{1}H NMR (400 MHz), δ, ppm: 1.13 (t, J = 7.9 Hz, 6H, CH_3(Et)), 1.16 (s, 18H, $CH_3(^tBu)$), 1.33 (q, J = 7.9 Hz, 4H, CH_2(Et)), 1.61 (s, 18H, $CH_3(^tBu)$), 6.74 (s, 2H, $CH_{quinone}$), 6.75 (m, 4H, CH(Ph)), 7.10 (m, 2H, CH(Ph)), 7.33 (m, 4H, CH(Ph)). ^{119}Sn NMR (149 MHz), δ, ppm: –202.10.

IR (ν, cm^{-1}): 1593 s, 1543 m, 1511 s, 1479 s, 1394 w, 1362 s, 1337 s, 1292 s, 1269 s, 1220 s, 1200 w, 1176 s, 1070 m, 1011 w, 953 w, 931 w, 918 w, 908 w, 898 w, 838 w, 820 w, 795 w, 765 сл, 739 w, 697 m, 686 w, 653 w, 613 w, 604 w, 576 w, 545 w, 521 w.

Complex $L_2Sn(^nBu)_2$ (**V**): analytically pure complex **V** was obtained in a yield of 0.32 g (75%).

For $C_{44}H_{58}N_2O_4Sn$

anal. calcd., %	C, 67.53	H, 7.79	N, 3.28	Sn, 13.90
Found, %	C, 67.56	H, 7.81	N, 3.26	Sn, 13.86

^{1}H NMR (400 MHz), δ, ppm: 0.83 (t, J = 7.23 Hz, 6H, $CH_3(^nBu)$), 1.16 (s, 18H, $CH_3(^tBu)$), 1.33 (m, 8H, $CH_2(^nBu)$), 1.48 (m, 4H, $CH_2(^nBu)$), 1.61 (s, 18H, $CH_3(^tBu)$), 6.74 (s, 2H, $CH_{quinone}$), 6.75 (m, 4H, CH(Ph)), 7.10 (m, 2H, CH(Ph)), 7.34 (m, 4H, CH(Ph)). ^{119}Sn NMR (149 MHz), δ, ppm: –199.04.

IR (ν, cm^{-1}): 1596 s, 1555 w, 1521 s, 1480 s, 1394 m, 1360 s, 1340 s, 1299 s, 1268 s, 1230 w, 1219 s, 1201 m, 1176 s, 1072 m, 1013 w, 959 w, 933 w, 928 w, 912 m, 900 w, 877 w, 850 w, 836 w, 818 w, 796 w, 764 w,

735 m, 696 s, 651 w, 621 m, 606 w, 576 w, 544 w, 533 w, 520 w.

Complex $L_2Sn(^tBu)_2$ (**VI**): analytically pure complex **VI** was obtained in a yield of 0.29 g (68%).

For $C_{44}H_{58}N_2O_4Sn$

Anal. calcd., %	C, 67.53	H, 7.79	N, 3.28	Sn, 13.90
Found, %	C, 67.58	H, 7.80	N, 3.25	Sn, 13.85

^{1}H NMR (400 MHz), δ, ppm: 1.17 (s, 18H, $CH_3(^tBu)$), 1.20 (s, 18H, $CH_3(^tBu)$), 1.61 (s, 18H, $CH_3(^tBu)$), 6.75 (m, 4H, CH(Ph)), 6.76 (s, 2H, $CH_{quinone}$), 7.10 (m, 2H, CH(Ph)), 7.33 (m, 4H, CH(Ph)).

IR (ν, cm^{-1}): 1588 s, 1551 m, 1521 s, 1511 m, 1480 s, 1392 s, 1359 s, 1336 s, 1298 s, 1264 s, 1220 s, 1203 m, 1174 s, 1162 s, 1070 s, 1023 w, 1010 m, 958 w, 929 w, 912 m, 898 m, 837 w, 818 w, 804 w, 796 w, 766 w, 734 m, 696 s, 652 w, 628 m, 616 w, 603 w, 573 w, 535 w, 517 w.

Complex L_2SnPh_2 (**VII**): analytically pure complex **VII** was obtained in a yield of 0.384 g (86%).

For $C_{52}H_{58}N_2O_4Sn$

Anal. calcd., %	C, 69.88	H, 6.54	N, 3.13	Sn, 13.28
Found, %	C, 69.92	H, 6.56	N, 3.11	Sn, 13.24

^{1}H NMR (400 MHz), δ, ppm: 1.02 (s, 18H, $CH_3(^tBu)$), 1.67 (s, 18H, $CH_3(^tBu)$), 6.69 (s, 2H, $CH_{quinone}$), 6.70 (m, 4H, CH(Ph)), 7.13 (m, 2H, CH(Ph)), 7.33–7.42 (m, 4H, CH(Ph) + m, 6H, CH(Ph)), 7.80 (m, 4H, CH(Ph)). ^{119}Sn NMR (149 MHz), δ, ppm: –340.76.

IR (ν, cm^{-1}): 1581 s, 1567 s, 1551 m, 1514 w, 1478 m, 1430 w, 1395 w, 1363 m, 1333 m, 1295 s, 1266 m, 1219 m, 1179 m, 1072 w, 1010 w, 998 w, 930 w, 914 w, 897 w, 837 w, 819 w, 796 w, 765 w, 739 w, 731 m, 696 m, 659 w, 623 w, 603 w, 575 w, 562 w, 520 w, 494 w.

X-ray diffraction analyses for complexes I and IV. Single crystals of the complexes suitable for X-ray diffraction analysis were obtained from methanol and diethyl ether, respectively. X-ray diffraction analyses were carried out on Smart Apex (**I**) and BrukerD8 Quest (**IV**) diffractometers (MoK_α radiation, graphite monochromator) at 100(2) K. The structures of compounds **I** and **IV** were solved by a direct method followed by the refinement by full-matrix least squares for F^2 (SHELXTL) [12]. An absorption correction was applied using the SCALE3 ABSPACK program [13]. All non-hydrogen atoms were refined in the anisotropic approximation. Hydrogen atoms were placed in the geometrically calculated positions and refined in the riding model. The crystallographic data and the main refinement parameters are given in Table 1. Selected bond lengths and bond angles in the molecules of complexes **I** and **IV** are listed in Table 2.

The crystallographic data for the complexes were deposited with the Cambridge Crystallographic Data Centre (CIF files CCDC no. 1557840 (**I**) and 1557839 (**IV**); deposit@ccdc.cam.ac.uk or http://www.ccdc.cam.ac.uk/data_request/cif).

RESULTS AND DISCUSSION

As in the case of similar compounds based on L'H described earlier [8], the tin complexes based on 2-hydroxy-*p*-iminobenzoquinone (**I–VII**) are formed in the exchange reactions between potassium salt LK and the corresponding organotin chlorides in methanol (Scheme 1). The compounds are isolated from the reaction mixture as finely crystalline intensively vinous-colored substances.

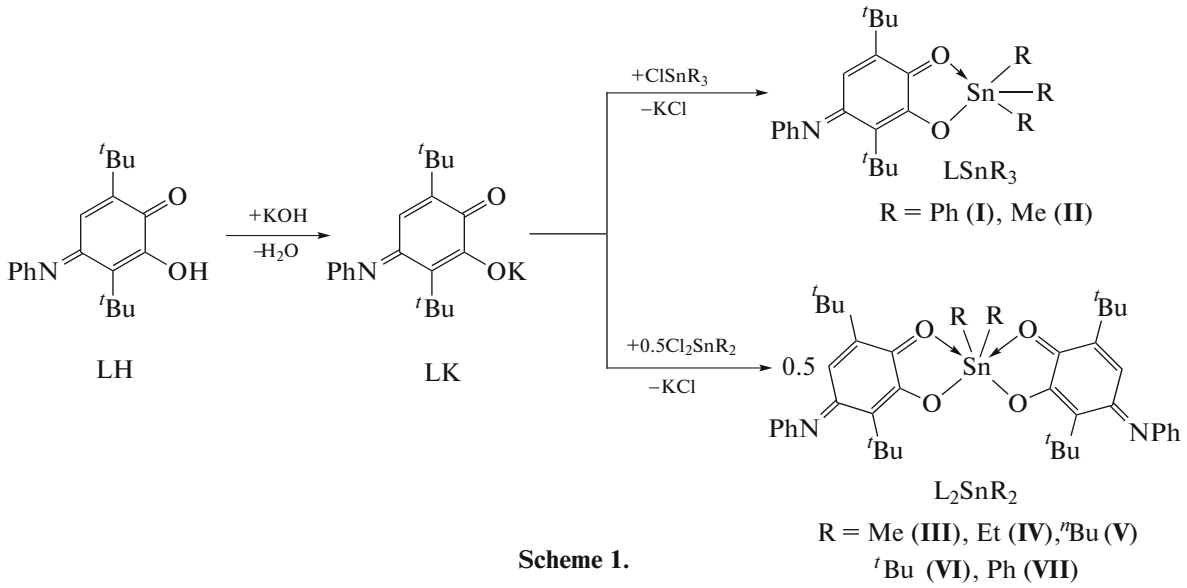

Scheme 1.

The compositions and structures of the synthesized complexes were determined using a series of physicochemical methods (elemental analysis, IR spectroscopy, and ^{1}H and ^{119}Sn NMR spectroscopy). X-ray diffraction analyses were carried out for compounds **I** and **IV**.

The structure of complex **I** (Fig. 1a) differs from those of the earlier studied related compounds of trimethyl- and triphenyltin(IV) based on the 2-oxy-3,6-di-*tert*-butyl-*p*-benzoquinone ligand [8, 10]. The molecules of the latter in crystal are linked to form uniform chains by donor–acceptor bonds between the metal center and oxygen atom of the adjacent molecule. The coordination number of the tin atom is six. In complex **I** based on the 2-oxy-*p*-iminobenzoquinone ligand, the N(1) atom is shielded by the phenyl ring, which impedes the formation of a donor–acceptor bond with the metal atom of the adjacent molecule. The pentacoordinated tin atom in complex **I** exists in the distorted trigonal bipyramidal coordination. The base of the bipyramid is formed by the O(1), C(21), and C(27) atoms, and the O(2) and C(33) atoms are located in the axial vertices. The tin atom shifts from the plane of the bipyramid base by 0.399 Å. The O(2)Sn(1)C(33) angle is 161.75(5)°. The Sn(1)–O(1) bond (2.0443(11) Å) is covalent. The Sn(1)–O(2) distance (2.5147(11) Å) significantly exceeds the sum of covalent radii of the corresponding elements (2.11 Å [14]), indicating the donor–acceptor nature of this bond. The considered distances in complex **I** are substantially shorter than the corresponding bonds in similar tin compounds based on the 2-hydroxy-*p*-benzoquinone ligand [8, 10] and, as a consequence, they should be stronger. The C(1)–O(1)

Table 1. Crystallographic data and X-ray diffraction experimental and refinement parameters for complexes **I** and **IV**

Parameter	Value	
	$LSnPh_3$ (**I**)	L_2SnEt_2 (**IV**)
FW	660.39	797.61
Temperature, K	100(2)	100(2)
Crystal system	Monoclinic	Triclinic
Space group	$P2_1/n$	$P\overline{1}$
a, Å	10.5569(6)	10.3305(14)
b, Å	19.2464(11)	10.6074(14)
c, Å	15.5947(9)	19.970(3)
α, deg	90	101.529(3)
β, deg	92.0480(10)	91.001(3)
γ, deg	90	104.339(3)
V, Å^3	3166.5(3)	2072.2(5)
Z	4	2
F(000)	1360	836
ρ_{calcd}, g cm^{-3}	1.385	1.278
μ, mm^{-1}	0.841	0.658
Crystal size, mm	0.50 × 0.20 × 0.20	0.18 × 0.12 × 0.10
Measurement range over θ, deg	1.68–26.00	2.225–29.999
Ranges of reflection indices	$-13 \le h \le 13$, $-23 \le k \le 23$, $-19 \le l \le 19$	$-14 \le h \le 14$, $-14 \le k \le 14$, $-28 \le l \le 28$
Number of observed reflections	26813	31421
Number of independent reflections	6213	12033
R_{int}	0.0180	0.0208
Goodness-of-fit (F^2)	1.054	1.057
R_1, wR_2 ($I > 2\sigma(I)$)	0.0211, 0.0553	0.0226, 0.0563
R_1, wR_2 (for all reflections)	0.0229, 0.0561	0.0253, 0.0573
Residual electron density (max/min), *e* Å^{-3}	0.715/–0.231	0.826/–0.297

Table 2. Selected bond lengths (Å) and angles (deg) in complexes **I** and **IV**

Bond	*d*, Å	Bond	*d*, Å
		I	
Sn(1)–O(1)	2.0443(11)	C(3)–C(4)	1.337(2)
Sn(1)–O(2)	2.5147(11)	C(4)–C(5)	1.470(2)
C(1)–O(1)	1.3318(19)	C(5)–C(6)	1.475(2)
C(2)–O(2)	1.2405(19)	C(1)–C(6)	1.364(2)
C(5)–N(1)	1.295(2)	Sn(1)–C(21)	2.1270(16)
C(1)–C(2)	1.493(2)	Sn(1)–C(27)	2.1308(16)
C(2)–C(3)	1.476(2)	Sn(1)–C(33)	2.1511(16)
		IV	
Sn(1)–O(1)	2.0696(7)	C(1)–C(2)	1.4888(12)
Sn(1)–O(2)	2.4408(7)	C(2)–C(3)	1.4681(12)
Sn(1)–O(4)	2.4137(7)	C(3)–C(4)	1.3410(12)
Sn(1)–O(3)	2.0690(7)	C(4)–C(5)	1.4698(12)
Sn(1)–C(41)	2.1238(10)	C(5)–C(6)	1.4653(12)
Sn(1)–C(43)	2.1259(10)	C(1)–C(6)	1.3766(11)
C(1)–O(1)	1.3211(10)	C(21)–C(22)	1.5006(12)
C(2)–O(2)	1.2411(11)	C(22)–C(23)	1.4647(11)
C(22)–O(4)	1.2390(11)	C(23)–C(24)	1.3388(13)
C(21)–O(3)	1.3218(10)	C(24)–C(25)	1.4702(13)
C(5)–N(1)	1.3004(11)	C(25)–C(26)	1.4695(12)
C(35)–N(2)	1.3009(12)	C(21)–C(26)	1.3749(13)
Angle	ω, deg	Angle	ω, deg
		I	
O(1)Sn(1)C(21)	110.88(5)	C(27)Sn(1)C(33)	104.57(6)
O(1)Sn(1)C(27)	120.31(5)	O(1)Sn(1)O(2)	68.86(4)
C(21)Sn(1)C(27)	118.18(6)	C(21)Sn(1)O(2)	82.73(5)
O(1)Sn(1)C(33)	92.89(5)	C(27)Sn(1)O(2)	85.38(5)
C(21)Sn(1)C(33)	105.05(6)	C(33)Sn(1)O(2)	161.75(5)
		IV	
O(3)Sn(1)O(1)	82.27(2)	C(41)Sn(1)O(4)	85.61(3)
O(3)Sn(1)C(41)	102.95(4)	C(43)Sn(1)O(4)	80.41(3)
O(1)Sn(1)C(41)	103.08(3)	O(3)Sn(1)O(2)	152.36(2)
O(3)Sn(1)C(43)	104.70(3)	O(1)Sn(1)O(2)	70.22(2)
O(1)Sn(1)C(43)	105.20(3)	C(41)Sn(1)O(2)	81.34(3)
C(41)Sn(1)C(43)	142.57(4)	C(43)Sn(1)O(2)	85.66(3)
O(3)Sn(1)O(4)	70.48(2)	O(4)Sn(1)O(2)	137.10(2)
O(1)Sn(1)O(4)	152.66(2)		

bond (1.3318(19) Å) is typically ordinary, whereas the C(2)–O(2) (1.2405(19) Å) and C(5)–N(1) (1.295(2) Å) distances are characteristic of double bonds. As in the previously studied monooxy-*p*-benzoquinone tin complexes [8, 10], the coordination of the O(2) atom with the metal center in complex **I** does not result in the elongation of the C=O double bond. The double and ordinary C–C bonds alternate in the six-membered carbon cycle of the monooxy-*p*-iminobenzoquinone ligand. The C(3)–C(4) (1.337(2) Å) and C(1)–C(6) (1.364(2) Å) bonds are separated by two ordinary bonds C(1)–C(2), C(2)–C(3), C(4)–C(5), and C(5)–C(6) (1.470(2)–1.493(2) Å).

The structure of bis(ligand) complex **IV** resembles that of the earlier studied similar tin compound containing two monooxy-*p*-benzoquinone ligands and two *n*-butyl groups at the metal atom [8]. The hexacoordinated tin atom in compound **IV** exists in a strongly distorted octahedral ligand environment (Fig. 1b). The C(41), O(2), O(3), and C(44) atoms form the base of the octahedron, and the O(1) and O(4) atoms are in the apical positions. The O(1)Sn(1)O(4) angle strongly deviates from 180° and is equal to 152.66(2)°. The octahedron base is also strongly distorted, and the OSnC angles substantially differ from 90°. The tin atom lies almost in the O(1)O(2)O(3)O(4) plane (shifts from the plane by 0.007 Å only). The both chelating monooxy-*p*-iminobenzoquinone ligands are nearly planar, and the dihedral angle between their planes is 8.61°. The ethyl groups at the metal atom are in the *cis* position relative to each other. Ligands L are arranged in such a way that the carbonyl O(2) and O(4) atoms and imine N(1) and N(2) atoms are also in the *cis* position, and the O(2)Sn(1)O(4) and O(1)Sn(1)O(3) angles are 137.10(2)° and 82.27(2)°, respectively. The bond length distribution in complex **IV** (in particular, in ligands L) resembles that in the above considered compound **I** and in the known tin derivatives based on the monooxy-*p*-benzoquinone ligand [8, 10]. The Sn(1)–O(1) and Sn(1)–O(3) bond lengths (2.0696(7) and 2.0690(7) Å) are significantly less than the sum of covalent radii of the corresponding elements (2.11 Å [14]), indicating their covalent nature. On the contrary, the Sn(1)–O(2) (2.4408(7) Å) and Sn(1)–O(4) (2.4137(7) Å) distances exceed the sum of covalent radii of tin and oxygen by more than 0.3 Å but are less than the sum of their van der Waals radii (3.7 Å [14]). Thus, these bonds are donor–acceptor. The C(1)–O(1) (1.3211(10) Å) and C(21)–O(3) (1.3218(10) Å) distances are shorter than the typical ordinary carbon–oxygen bonds in the phenolate [15] and catecholate complexes of tin(IV) [16, 17] and are close in value to those characteristic of the *o*-semiquinolate tin derivatives [18, 19]. At the same time, the C(2)–O(2) (1.2411(11) Å) and C(22)–O(4) (1.2390(11) Å) bonds are double. It should be mentioned that in complex **IV**, as in all studied complexes of this type, the appearance of a donor–acceptor interaction between the O(2) and O(4) oxygen atoms and the metal center upon complex formation does not result in the elongation of the C=O double bonds of the ligand. The *p*-quinoid distribution of double and ordinary bonds is retained in the six-membered carbon rings C(1)–C(6) and C(21)–C(26). The C(3)–C(4) (1.3410(12) Å) and C(1)–C(6) (1.3766(11) Å) bonds of one ring and C(23)–C(24) (1.3388(13) Å) and C(21)–C(26) (1.3749(13) Å) of another ring are separated by two ordinary bonds C(1)–C(2), C(2)–C(3), C(4)–C(5), and C(5)–C(6) (1.4653(12)–1.4888(12) Å) in the first ligand and C(21)–C(22), C(22)–C(23), C(24)–C(25), and C(25)–C(26) (1.4647(11)–1.5006(12) Å) in the second ligand.

The electrochemical behavior of free 2-hydroxy-*p*-iminobenzoquinone and related tin(IV) complexes in a dichloromethane solution at the GC electrode was studied by the CV method (Table 3). The electrochemical reduction of LH proceeds in two irreversible steps (Fig. 2). The fast chemical step occurs in a solution after the transfer of one electron. The reoxidation peaks (–0.30 and 0.26 V) of the chemical reaction products are detected in the inverse branch of the CV curve. Since the generated radical-anionic species (monohydroxy-*p*-iminobenzoquinones) are highly basic, the protonation reaction with monoanion formation occurs in a solution (Scheme 2).

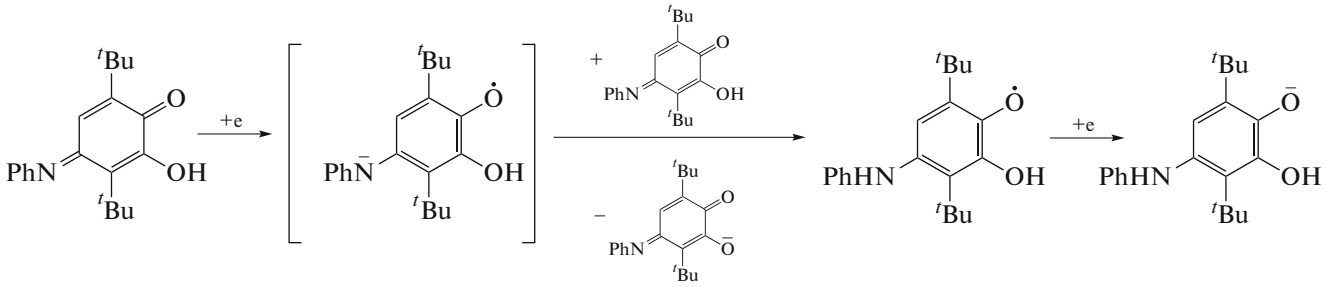

Scheme 2.

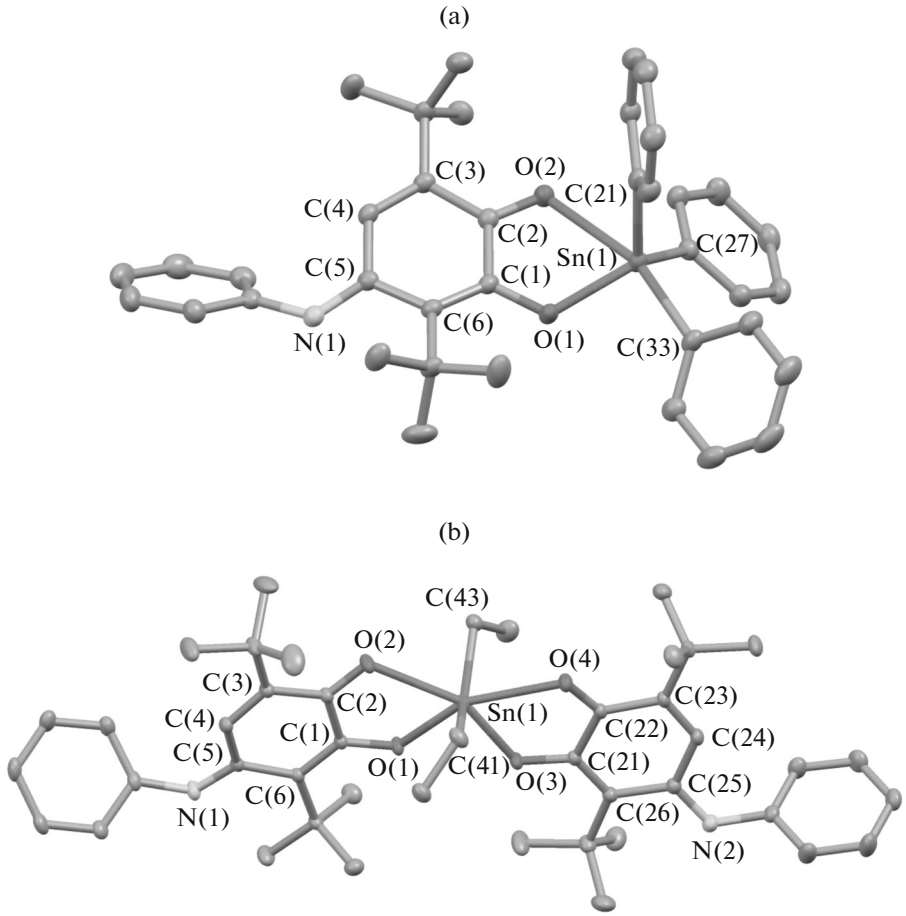

Fig. 1. Molecular structures of complexes (a) **I** and (b) **IV**. Thermal ellipsoids are presented with 50% probability. Hydrogen atoms are omitted.

The reduction of sterically hindered *o*-iminobenzoquinones is also irreversible and affords the corresponding monoanion [20]. In the case considered, the proton source is the hydroxy group of the second LH molecule acting as an internal donor. A similar behavior was observed for 2-hydroxy-1,4-naphthoquinones [21, 22]. The phenoxyl radical is formed due to protonation (Scheme 2). The peak at a potential of –0.34 V is detected in the inverse branch of the voltammogram. This peak can equally correspond to the oxidation of both the phenoxyl radical and singly deprotonated form of completely reduced *p*-iminobenzoquinone. The formation of the monoanion in a solution is explained by the possibility of the generated phenoxyl radical to be reduced in the same potential range either at the electrode due to the heterogeneous electron transfer, or in the course of the chemical reaction in a solution (disproportionation). The first cathodic peak is lower in current than the one-electron level, which indicates the participation of some amount of the starting monohydroxy-*p*-iminobenzoquinone in the redox reactions, in particular, in protonation.

The second cathodic process has a one-electron irreversible character. To establish its nature, we studied the electrochemical behavior of 2-hydroxy-*p*-iminobenzoquinone in the presence of a base, tetrabutylammonium hydroxide (alcohol solution), in acetonitrile. The reduction of the starting ligand LH in acetonitrile proceeds similarly to the described above processes in dichloromethane: two cathodic peaks at –0.69 and –1.40 V are observed in the CV curves. The one-electron irreversible peak is detected at a potential of –1.40 V in the presence of the base, which coincides with the data on the electrochemical reduction of LH in acetonitrile. Therefore, the second cathodic process is related to the reduction of the monohydroxy-*p*-iminobenzoquinone monoanion formed in the near-electrode range during deprotonation. The peak at –0.35 V detected in the inverse branch of the voltammogram corresponds to the oxidation of the chemical reaction product following the electron transfer, since only the oxidation peak of the monohydroxy-*p*-iminobenzoquinone monoanion is detected at 0.26 V for the potential sweep from –0.7 to +0.7 V. The radical dianion generated by the reduction of the monoanion

Table 3. Electrochemical potentials for the studied compounds according to the CV method*

Compound	E^1_{red}, V**	E^2_{red}, V	E^3_{red}, V	E^1_{ox}, V	E^2_{ox}, V**
LH	–0.77	–1.51		1.47	1.67
L'H***	–0.57	–1.51 (–1.44)		1.96	
I	–0.70	–1.52 (–1.46)		1.48	1.60
L'$SnPh_3$***	(–0.47)	(–1.44)		1.82	
III	–0.66	–1.11 (–1.06)	–1.49 (–1.41)	1.29	1.44
IV	–0.77	–1.15 (–1.09)	–1.52 (–1.42)	1.30	1.52
V	–0.79	–1.16	–1.53 (–1.45)	1.28	1.54
VI	–0.79 (–0.74)	–1.17 (–1.13)	–1.51 (–1.43)	1.25	1.50 1.61
VII	–0.62	–1.09 (–1.03)	–1.51 (–1.42)	1.46	1.57

* CH_2Cl_2, GC anode, $V = 0.2$ V/s, vs. Ag/AgCl/KCl, 0.1 M NBu_4ClO_4, $c = 0.001–0.003$ mol/L, argon.
** E_{red} and E_{ox} are the reduction and oxidation potentials, respectively; the reduction half-wave potentials for the quasi-reversible cathodic processes are given in parentheses.
*** Published data [8].

can be reduced further at more cathodic potentials or can disproportionate. In addition, being a strong base, the radical dianion is capable of proton detaching (from alcohol under the given conditions), which can result in the formation of both radical-anionic species and monoanion.

The electrochemical transformation of 2-hydroxy-3,6-di-*tert*-butyl-*p*-benzoquinone (L'H) was described [8]. The second cathodic process was ascribed to phenoxyl radical reduction. In this work, we studied the electrochemical behavior of L'H in acetonitrile in the presence of the base (tetrabutylammonium hydroxide). It turned out that the electrochemical reduction of the studied *p*-iminobenzoquinone and *p*-benzoquinone proceeded, under these conditions, via a similar mechanism: for L'H, a cathodic peak is detected at –1.41 V in the CV curve upon the addition of one equivalent of the base and is nearly identical to the peak observed for LH under similar conditions. Therefore, in the case of L'H, the second cathodic process corresponds in fact to the reduction of the *p*-benzoquinone monoanion.

The data obtained (Table 3) show that the replacement of the oxygen atom in monohydroxy-*p*-benzoquinone by the nitrogen atom results in the shift of the first cathodic peak to the range of more negative

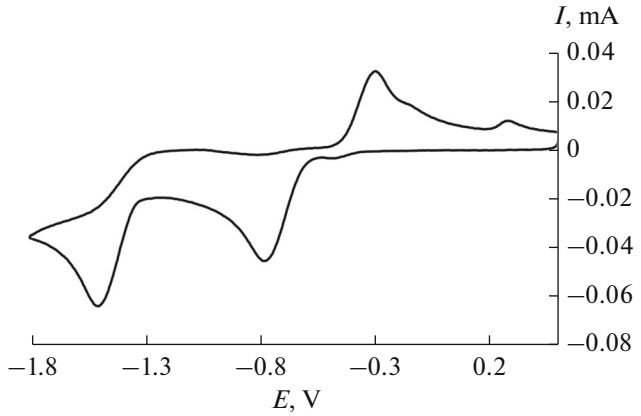

Fig. 2. CV curves for the reduction of LH (CH_2Cl_2, GC anode, Ag/AgCl/KCl, 0.1 M NBu_4ClO_4, $c = 3 \times 10^{-3}$ mol/L, argon).

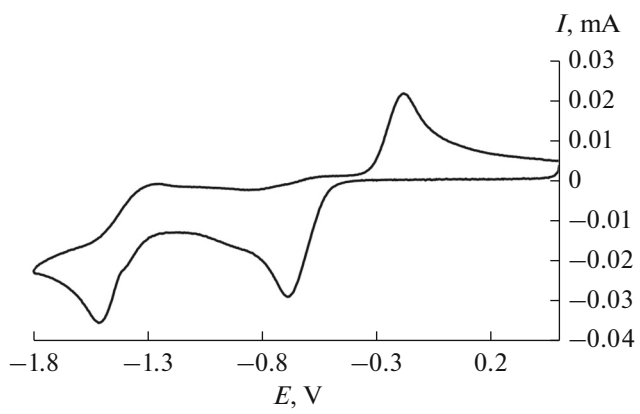

Fig. 3. CV curve for the reduction of complex **I** (CH_2Cl_2, GC anode, Ag/AgCl/KCl, 0.1 M NBu_4ClO_4, $c = 3 \times 10^{-3}$ mol/L, argon).

potentials and the reduction potentials of the *p*-iminobenzoquinone and *p*-benzoquinone monoanions are comparable.

The electrochemical behavior of 2-hydroxy-*p*-iminobenzoquinone in the presence of a strong acid (methanetrifluorosulfonic acid) was studied. The protonation of LH, as in the case of sterically hindered *o*-iminobenzoquinones [20], results in the shift of the reduction potential to the anodic range (0.31 V), and the process becomes two-electron. The anodic peak corresponding to the oxidation of completely reduced monohydroxy-*p*-iminobenzoquinone is detected at 0.64 V in the inverse branch of the voltammogram.

The electrochemical oxidation of LH in dichloromethane (1.47 V) and acetonitrile (1.35 V) proceeds irreversibly and corresponds to imino group oxidation. The detected value of the oxidation potential is close to those obtained earlier for *o*-iminobenzoquinones [20]. Additional irreversible oxidation peaks are detected at higher anodic potentials in the CV curve (Table 3).

The electrochemical reduction of complex **I** differs significantly from that for the similar compound based on the monooxy-*p*-benzoquinone ligand L'$SnPh_3$ [8]. In the case of complex **I**, the first redox transition is irreversible and the second transition is quasi-reversible (Fig. 3), whereas two consecutive quasi-reversible one-electron reduction steps were observed for the *p*-benzoquinone derivative of tin(IV) [8]. The reoxidation peak of the product of the chemical reaction following the electron transfer is detected in dichloromethane in the inverse branch of the CV curve. The peak current increases with the potential sweep covering the second cathodic step, which indicates an increase in the concentration of the formed intermediate product. No similar changes were observed in the voltammograms for the tin(IV) derivatives based on 2-hydroxy-*p*-benzoquinone [8]. The following mechanism of electrochemical transformations can be proposed for L$SnPh_3$ (Scheme 3).

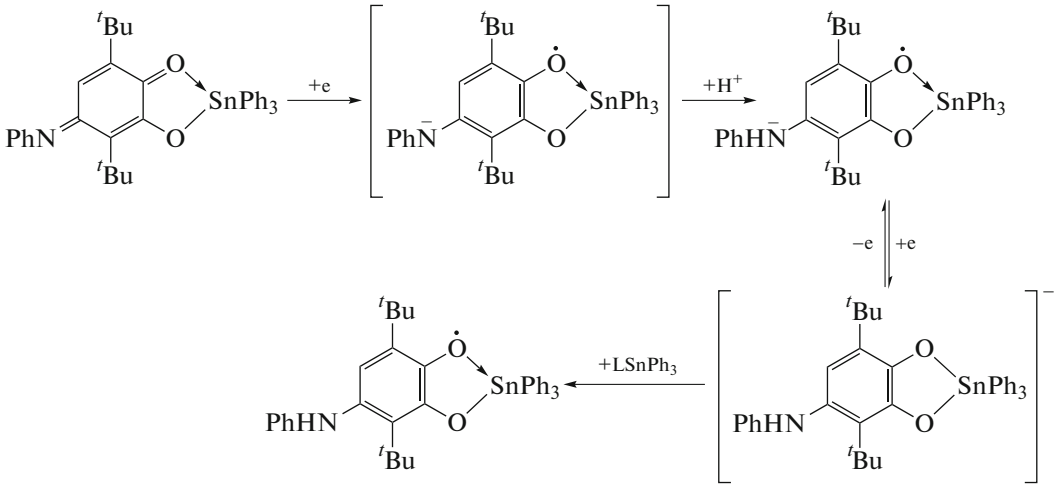

Scheme 3.

The electrochemical reduction in the first step results in the formation of an unstable radical-anionic species, which is subjected to protonation due to the high basicity. The coordinatively bound phenoxyl radical is more stable and is reduced quasi-reversibly (I_a/I_c = 0.5) to the corresponding dianion, which is rapidly oxidized in the near-electrode range by the starting molecules of the complex, also leading to the overestimation of the current of the first cathodic peak.

The electrochemical oxidation of complex **I** proceeds in two irreversible steps at the potentials (Table 3) close to those obtained for the free ligand, which assumes the involvement of the imino group into the anodic process.

The electrochemical reduction of complexes **III–VII** proceeds in different manners, and the organic groups at the tin(IV) atom exert a significant effect on the redox behavior (Table 3). For complexes **III–V**, the first cathodic step is irreversible and corresponds to the reduction of one of the ligands followed by protonation (Fig. 4). A poorly pronounced cathodic peak, possibly corresponding to the reduction of the second ligand, is detected at the potential from −1.15 to −1.17 V. Then, at the potential sweep to the cathodic range, a quasi-reversible cathodic peak is observed in the range from −1.51 to −1.54 V, which is close in value to the

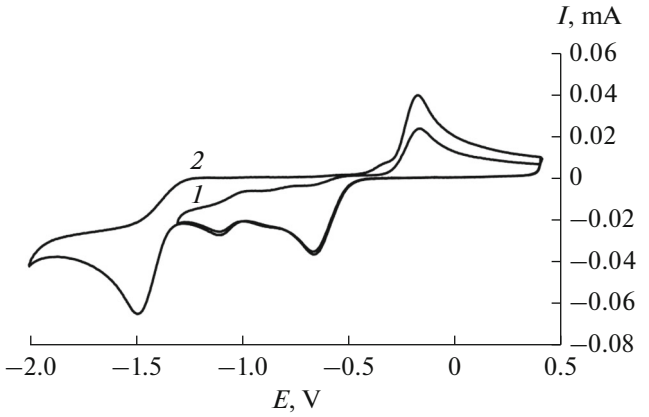

Fig. 4. CV curves for the reduction of complex L_2SnMe_2 (**III**) (potential sweep: (*1*) 0.4 to −1.3V and (*2*) 0.4 to −2.0 V; CH_2Cl_2, GC anode, Ag/AgCl/KCl, 0.1 M NBu_4ClO_4, $c = 3 \times 10^{-3}$ mol/L, argon).

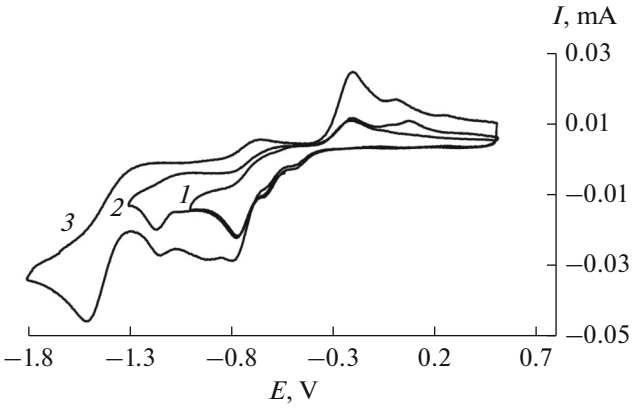

Fig. 5. CV curves for the reduction of complex $L_2Sn(^tBu)_2$ (**VI**) (potential sweep: (*1*) 0.5 to −1.0 V, (*2*), 0.5 to −1.30 V, and (*3*) 0.5 to −1.8 V; CH_2Cl_2, GC anode, Ag/AgCl/KCl, 0.1 M NBu_4ClO_4, $c = 3 \times 10^{-3}$ mol/L, argon).

data obtained for LH and monoligand complex **I**. For complexes **III–VII**, reoxidation peaks were detected in the range from −0.19 to −0.24 V in the reverse scans of the voltammograms, whose potentials differed from each other depending on the nature of organic groups at the tin atom.

Two irreversible oxidation peaks are detected in the anodic range for complexes **III–V**. The peak potentials for the first anodic process are independent of the substituents at the tin atom.

The behavior of complexes **VI** and **VII** differs from that of the above considered bis(ligand) compounds. For complex **VI**, the first redox transition is quasi-reversible, but the generated radical-anionic intermediate is poorly stable ($I_a/I_c = 0.5$) and is subjected to chemical transformations in a solution (Fig. 5). Steric shielding by the *tert*-butyl groups favors the partial stabilization of the formed monoanionic complex. The second quasi-reversible process becomes more pronounced. The following scheme of redox transformations of complex **VI** can be proposed for the first two cathodic steps (Scheme 4).

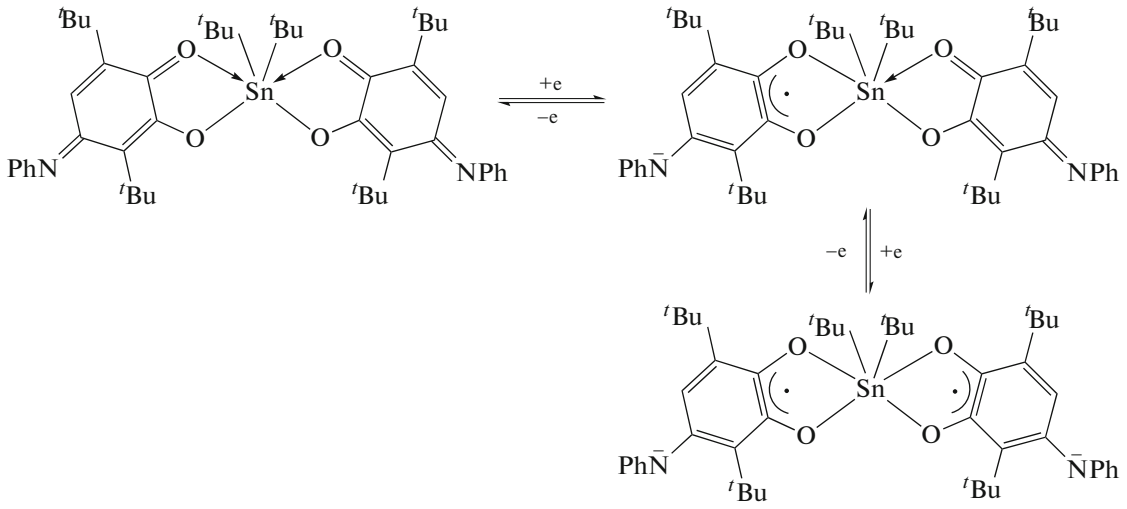

Scheme 4.

The third quasi-reversible step insignificantly exceeds in current the one-electron level. After the third redox process, the reduced species of the ligands are reduced in a solution, resulting in an increase in

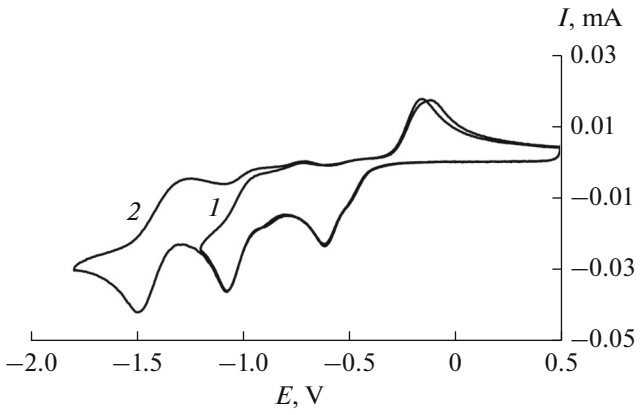

Fig. 6. CV curves for the reduction of complex L_2SnPh_2 (**VII**) (potential sweep: (*1*) 0.5 to −1.2 V and (*2*) 0.5 to −1.8 V; CH_2Cl_2, GC anode, Ag/AgCl/KCl, 0.1 M NBu_4ClO_4, $c = 1 \times 10^{-3}$ mol/L, argon).

the current of the reoxidation peak in the inverse branch of the voltammogram. For complex **VI**, the first anodic process is observed at the potential (1.24 V) insignificantly shifted to the cathodic range compared to complexes **III–V**, and the second oxidation step is split into two peaks (Table 3).

Compound **VII** differs from the complexes of the whole series, because its reduction potential is shifted to the anodic range, which is due to the influence of the phenyl groups at the metal atom. The second cathodic step is pronounced and has a one-electron character (Fig. 6). As a result of the first redox transition, the *p*-iminosemiquinolate tin derivative is formed and further undergoes protonation in a solution. The second redox process becomes quasi-reversible. The reoxidation peak at −0.16 V in the inverse branch of the voltammogram is similar to the peak detected in the case of complex **I** (Fig. 3). The values of reduction potentials for the first and second steps are shifted to the cathodic range by 0.33–0.35 V compared to the similar tin compound based on the 2-hydroxy-*p*-benzoquinone ligand [8]. The third cathodic step is also quasi-reversible, and its potential is close to the reduction potential of the free monoanion of LH.

The electrochemical oxidation of complex **VII** proceeds in two steps: the potential of the first redox transition is shifted to the anodic range by 0.15–0.16 V compared to compounds **III–V**, and the second step is detected at the potentials close to those for compounds **III–V**.

To conclude, it is shown by the performed electrochemical studies that LH is reduced with the formation of the corresponding monoanion, which was generated by using an organic base. In the case of compound **I**, the coordination of the phenoxyl radical formed due to the consecutive one-electron reduction and protonation to the tin atom favors its stabilization, which results in reversibility of the second step of the reduction of the complex. Unlike the earlier considered tin(IV) compounds based on 2-hydroxy-*p*-benzoquinone [8], complexes **III–V** are reduced irreversibly in the first step because of the high basicity of the generated monoanionic complex. The stability of the monoanionic complexes formed due to the cathodic processes is strongly affected by the hydrocarbon groups at the tin(IV) atom. The formation of a few mono- and dianionic complexes stable in the CV experiment time scale is detected for compound **VI** with *tert*-butyl groups. The redox behavior of complex **VII** is distinguished by a more pronounced character of the detected three one-electron cathodic steps compared to other studied compounds.

ACKNOWLEDGMENTS

This work was supported by the Russian Foundation for Basic Research (project no. 16-13-00027_mol_a) and the Council for Grants of the President of the Russian Federation (project for support of leading scientific schools NSh-7916.2016.3).

REFERENCES

1. Kaim, W. and Schwederski, B., *Coord. Chem. Rev.*, 2010, vol. 254, nos. 13–14, p. 1580.
2. Kaim, W., *Inorg. Chem.*, 2011, vol. 50, no. 20, p. 9752.
3. Kaim, W., *Eur. J. Inorg. Chem.*, 2012, vol. 2012, no. 3, p. 343.
4. Luca, O.R. and Crabtree, R.H., *Chem. Soc. Rev.*, 2013, vol. 42, no. 4, p. 1440.
5. Broere, D.L.J., Plessius, R., and Vlugt, J.I., *Chem. Soc. Rev.*, 2015, vol. 44, no. 19, p. 6886.
6. Jacquet, J., Blanchard, S., Derat, E., et al., *Chem. Sci.*, 2016, vol. 7, no. 3, p. 2030.
7. Jacquet, J., Salanouve, E., Orio, M., et al., *Chem. Commun.*, 2014, vol. 50, no. 72, p. 10394.
8. Piskunov, A.V., Meshcheryakova, I.N., Fukin, G.K., et al., *Russ. J. Coord. Chem.*, 2014, vol. 40, no. 4, p. 205.
9. Khamaletdinova, H.M., Meshcheryakova, I.H., Piskunov, A.B., et al., *J. Struct. Chem.*, 2015, vol. 56, no. 2, p. 233.
10. Kabarova, N.Yu., Cherkasov, V.K., Zakharov, L.N., et al., *Izv. Akad. Nauk, Ser. Khim.*, 1992, no. 12, p. 2798.
11. Kocheshkov, K.A., in *Metody elementoorganicheskoi khimii. Germanii, olovo, svinets* (Methods of Heteroorganic Chemistry. Germanium. Tin. Lead), Moscow: Nauka, 1968, p. 704.
12. Sheldrick, G.M. *SHELXTL. Version 6.12. Structure Determination Software Suite*, Madison: Bruker AXS, 2000.
13. SCALE3 ABSPACK. Empirical Absorption Correction Using Spherical Harmonics. CrysAlisPro, Agilent Technologies.
14. Batsanov, S.S., *Zh. Neorg. Khim.*, 1991, vol. 36, no. 12, p. 3015.

15. Jurkschat, K., Pieper, N., Seemeyer, S., et al., *Organometallics*, 2001, vol. 20, no. 5, p. 868.
16. Lado, A.V., Piskunov, A.V., Cherkasov, V.K., et al., *Russ. J. Coord. Chem.*, 2006, vol. 32, no. 3, p. 173.
17. Piskunov, A.V., Lado, A.V., Fukin, G.K., et al., *Heteroatom. Chem.*, 2006, vol. 17, no. 6, p. 481.
18. Ilyakina, E.V., Poddel'sky, A.I., Piskunov, A.V., et al., *Inorg. Chim. Acta*, 2012, vol. 380, no. 1, p. 57.
19. Ilyakina, E.V., Poddel'sky, A.I., Piskunov, A.V., et al., *Inorg. Chim. Acta*, 2013, vol. 394, no. 1, p. 282.
20. Smolyaninov, I.V., Letichevskaya, N.N., Kulakov, A.V., et al., *Russ. J. Electrochem.*, 2007, vol. 43, no. 10, p. 1187.
21. Ferraz, P.A.L., Abreu, F.C., Pinto, A.V., et al., *J. Electroanalytic. Chem.*, 2001, vol. 507, nos. 1–2, p. 275.
22. Frontana, C., Frontana-Uribe, B.A., and Gonzalez, I., *J. Electroanalytic. Chem.*, 2004, vol. 573, no. 2, p. 307.

Translated by E. Yablonskaya